



Population Pharmacokinetic Study of Cefazolin Dosage Adaptation in Bacteremia and Infective Endocarditis Based on a Nomogram

✉ Ronan Bellouard,^{a,b} Colin Deschanvres,^{c,d} Guillaume Deslandes,^a Éric Dailly,^{a,b} Nathalie Asseray,^{c,d} Pascale Jolliet,^{a,e} David Boutoille,^{c,d,f} Benjamin Gaborit,^{c,d,f}  Matthieu Grégoire^{a,g}

^aClinical Pharmacology Department, Nantes University Hospital, Nantes, France

^bEE1701 Microbiotas, Hosts, Antibiotics and Bacterial Resistances, University of Nantes, Nantes, France

^cInfectious Diseases Department, Nantes University Hospital, Nantes, France

^dCIC 1413, INSERM, Nantes, France

^eUMR INSERM 1246 SPHERE Methods in Patients-Centered Outcomes and Health Research, University of Nantes, Nantes, France

^fEA 3826 Thérapeutiques Cliniques et Expérimentales des Infections, University of Nantes, Nantes, France

^gUMR INSERM 1235 The Enteric Nervous System in Gut and Brain Disorders, University of Nantes, Nantes, France

ABSTRACT Optimal dosing of continuous-infusion cefazolin can be challenging in patients being treated for bacteremia or infective endocarditis. The aim of this work is to describe and analyze the pharmacokinetics of cefazolin in those patients using a population pharmacokinetics modeling approach and to establish a nomogram to determine the optimal daily dose. Population pharmacokinetics were modeled using the Pmetrics package for R. Plasma concentrations were collected retrospectively from patients treated with continuous-infusion cefazolin for bacteremia or infective endocarditis. The influence of multiple parameters, including renal function, total body weight, body mass index, body surface area (BSA), ideal weight, lean body weight, height, and age, was tested. The probabilities of target attainment for selected target concentrations (40, 60, and 80 mg/liter) were calculated. A dosing nomogram was then developed, using the absolute value of the glomerular filtration rate (aGFR), to determine the optimal daily dose required to achieve the target concentrations in at least 90% of patients. In total, 346 cefazolin plasma concentrations from 162 patients were collected. A one-compartment model best described the data set. The only covariate was aGFR, calculated according to the Chronic Kidney Disease Epidemiology Collaboration (CKD-EPI) formula and the patient's body surface area, for the rate of elimination. Using the nomogram, achieving a cefazolin concentration target of 40 mg/liter with a success rate of at least 90% and with an aGFR of 30, 60, 90, and 120 ml/min requires a daily dose of 2.6, 4.3, 6.1, and 8.0 g/day, respectively. These results confirm the interest of posology adaptation of cefazolin according to aGFR.

KEYWORDS bacteremia, cefazolin, continuous infusion, infective endocarditis, nonparametric modeling, population pharmacokinetics

Staphylococcus aureus and other staphylococcal species are responsible for more than a quarter of bloodstream infections and infective endocarditis (1). The incidence of these pathologies has increased over the past few years, and these pathologies are associated with a high rate of mortality (a 15 to 25% mortality rate for adults with *S. aureus* bacteremia and a 20 to 30% mortality rate for adults with *S. aureus* endocarditis) (2). For methicillin-susceptible strains, treatment with antistaphylococcal penicillins, such as oxacillin or cloxacillin, is usually recommended (3, 4). However,

Citation Bellouard R, Deschanvres C, Deslandes G, Dailly É, Asseray N, Jolliet P, Boutoille D, Gaborit B, Grégoire M. 2019. Population pharmacokinetic study of cefazolin dosage adaptation in bacteremia and infective endocarditis based on a nomogram. *Antimicrob Agents Chemother* 63:e00806-19. <https://doi.org/10.1128/AAC.00806-19>.

Copyright © 2019 American Society for Microbiology. All Rights Reserved.

Address correspondence to Ronan Bellouard, ronan.bellouard@chu-nantes.fr.

Received 15 April 2019

Returned for modification 8 May 2019

Accepted 9 July 2019

Accepted manuscript posted online 15 July 2019

Published 23 September 2019

cefazolin appears to be an equally effective alternative for the treatment of *S. aureus* bacteremia (5, 6). For β -lactams, efficacy depends on the fraction of the time during the dosing interval in which the unbound concentration of the drug is maintained above the MIC ($fT_{>MIC}$) for the pathogenic bacteria. Positive clinical outcomes have been associated with ratios ranging from 50% $fT_{>MIC}$ to 100% $fT_{>4\times MIC}$ (7, 8). However, no study has investigated the clinical outcome versus the $fT_{>MIC}$ ratio for cefazolin specifically. In France, the recommended target plasma concentration for cefazolin (given as a continuous infusion or by intermittent administration) is 100% $fT_{>4\times MIC}$ for documented infections and 40 to 80 mg/liter (total fraction) for undocumented infections (9).

In guidelines, the recommended dosage for intravenous cefazolin is usually 6,000 mg daily for patients with normal renal function (3, 4). In France, recommendations are 80 to 100 mg/kg of body weight/day administered in 3 doses or by continuous infusion after a loading dose of 30 mg/kg over 1 h (<http://www.infectiologie.com/UserFiles/File/spilf/recos/2016-alternatives-penicillines-m-injectables.pdf>). For patients with impaired renal function, guidelines do not require precise adaptation of the dose but recommend it. Conversely, when renal clearance is markedly increased, such as in severe sepsis, β -lactam concentrations may be too low with the recommended dosage (10). *A priori* dose adaptation according to renal function seems to be necessary to anticipate the risk of under- or overdosing.

The aim of this study was to describe and analyze the pharmacokinetics of cefazolin administered by continuous infusion in patients treated for bacteremia and/or infective endocarditis using a nonparametric population pharmacokinetic modeling approach. We then sought to establish a dosing nomogram to determine the optimal daily dose of cefazolin to be administered based on the clinical and biological characteristics of the patient.

RESULTS

Patient characteristics and cefazolin concentrations. A total of 162 patients (129 with bacteremia and 33 with infective endocarditis) were included in the analysis. *S. aureus* was identified in 90.1% of the patients, *Staphylococcus epidermidis* was identified in 4.3% of the patients, and other species accounted for the remaining 5.6%. The median daily dose was 6,000 mg/day, and the dose range was from 500 mg/day to 12,000 mg/day. For patients with an absolute value of the glomerular filtration rate (aGFR) of ≥ 90 ml/min, the median daily dose was 7,000 mg/day and the dose range was from 3,000 mg/day to 12,000 mg/day. Eighty-six patients received a loading dose prior to the continuous infusion. Patient characteristics are summarized in Table 1.

A total of 346 cefazolin plasma concentrations were used for the pharmacokinetic analysis. The number of samples per patient ranged from 1 to 11. Nineteen concentrations from 7 patients were measured during a second hospitalization or after a prolonged interruption of the cefazolin treatment (range, 15 to 355 days after the start of the first treatment). Fifty-eight percent of cefazolin concentrations were measured from patients with an aGFR of < 90 ml/min, and 16% were measured from patients with an aGFR of > 120 ml/min. Blood sampling was done at least 12 h after the start of the treatment, except for 3 measurements. For 6 samples, measurement was done within 36 h after the interruption of the treatment to monitor the decrease in the plasma cefazolin concentration in patients displaying very high concentrations. All concentrations were above the lower limit of quantitation (LLOQ).

The first data set comprised 79 patients (227 concentrations), and the second data set comprised 83 patients (119 concentrations). Significant differences in the serum creatinine concentration, estimated glomerular filtration rate (eGFR), and aGFR were observed between the two groups (Table 1).

Population pharmacokinetics modeling. A comparison of the main candidate models is summarized in Table S1 in the supplemental material. The observed data were best described by a one-compartment structural model with the central compartment volume (V) and the elimination rate constant (K_e). More complex structural

TABLE 1 Summary of patient characteristics^a

Characteristic (unit)	Value		P value (significance)
	Patients for model development (n = 79)	Patients for model validation (n = 68)	
% of male patients	63	63	1.000
% of patients with infective endocarditis	24	18	0.330
Median (interquartile range):			
Age (yr)	70 (55–80)	65 (53–80)	0.240
Ht (cm)	170 (163–175)	168 (159–174)	0.074
Wt (kg)	73 (63–83)	74 (62–89)	0.750
BMI (kg/m ²)	26 (22–28)	27 (23–30)	0.208
LBW (kg)	62 (56–70)	60 (52–67)	0.054
IWR (kg)	61 (57–68)	59 (54–65)	0.042*
BSA (m ²)	1.83 (1.68–1.98)	1.84 (1.68–2.00)	0.967
Serum creatinine concn (μmol/liter)	79 (58–152)	69 (54–91)	0.0054*
eGFR (ml/min/1.73 m ²)	75.4 (34.8–103.9)	94.0 (66.9–106.8)	0.0070*
aGFR (ml/min)	73.5 (37.1–108.7)	95.9 (69.8–113.2)	0.0084*

^aBMI, body mass index is defined as weight/height², where weight is in kilograms and height is in meters; LBW, lean body weight, calculated with the Devine formula, which is 50 (if male) or 45.5 (if female) + 2.3 × [(height – 152.4)/2.54] (where height is in centimeters); IWR, ideal weight, calculated with the Robinson formula, which is 52 (if male) or 49 (if female) + 1.9 (if male) or 1.7 (if female) × [(height – 152.4)/2.54] (where height is in centimeters); BSA, body surface area, calculated with the Du Bois formula, which is 0.007184 × weight^{0.425} × height^{0.725} (where height is in centimeters); eGFR, estimated glomerular filtration rate, calculated with the CKD-EPI formula, which is 141 × [min(Scr/κ, 1)^α] × [max(Scr/κ, 1)^{–1.209}] × 0.993^{age} × 1.018 (if female) or 1.159 (if black), where Scr is the serum creatinine concentration, κ is 0.7 for females and 0.9 for males, α is –0.329 for females and –0.411 for males, min indicates the minimum of Scr/κ or 1, and max indicates the maximum of Scr/κ or 1; aGFR, absolute value of the glomerular filtration rate, which is calculated as (eGFR × BSA)/1.73. Qualitative characteristics were compared using a two-tailed Fisher’s exact test, and quantitative data were compared using a Mann-Whitney-Wilcoxon test. Statistically significant results are marked with an asterisk.

models did not significantly improve the Akaike information criterion (AIC), population bias, or imprecision. One covariate was found to have an influence on the model parameters: the aGFR normalized with the dataset median on K_e . The relationship was best described by a power equation, $K_e = (aGFR/64)^{K_e1}$. The final structural model is represented in Fig. S1, and pharmacokinetic parameters estimates are summarized in Table 2. A lambda error model with a starting value of 7.5 was chosen, and values for error coefficients C_0 , C_1 , C_2 , and C_3 were 2.5, 0.15, 0, and 0, respectively, for the standard deviation (SD) polynomial. The final cycle value of lambda was 10.2, which indicates some process noise due to the retrospective nature and heterogeneity of the data.

Observation-versus-prediction plots are presented in Fig. 1. Bias and imprecision were 0.096 and 1.44, respectively, for population predictions and –0.076 and 0.51, respectively, for individual predictions. Residual plots for population predictions showed an even distribution of weighted residual errors over the concentration range and over time (Fig. S2).

Model validation. Visual predictive check (VPC) and prediction-corrected visual predictive check (pcVPC) plots revealed that the model correctly described the observed data (Fig. 2). Some variability could be observed for low values of aGFR, due to the heterogeneity of the data, covariate influence, and population variability.

TABLE 2 Population parameters estimates^a

Parameter	Estimation	Range
K_e1		
Median (95% CI)	0.907 (0.755–1.171)	0.01–3.00
MAWD (95% CI)	0.152 (0.000–0.286)	
V		
Median (95% CI)	3.193 (3.156–4.023)	1–15
MAWD (95% CI)	0.342 (0.000–0.867)	

^aIn the model, $K_e = (aGFR/64)^{K_e1}$, where K_e is the elimination rate constant from the central compartment (in hours^{–1}), aGFR/64 is the absolute estimate of the glomerular filtration rate (in milliliters per minute) normalized to the dataset median, and K_e1 is the power factor used to scale aGFR to the elimination rate constant. CI, confidence interval; MAWD, median absolute weighted deviation, used as an estimate of the variance for a nonparametric distribution; V, volume of the central compartment (in liters).

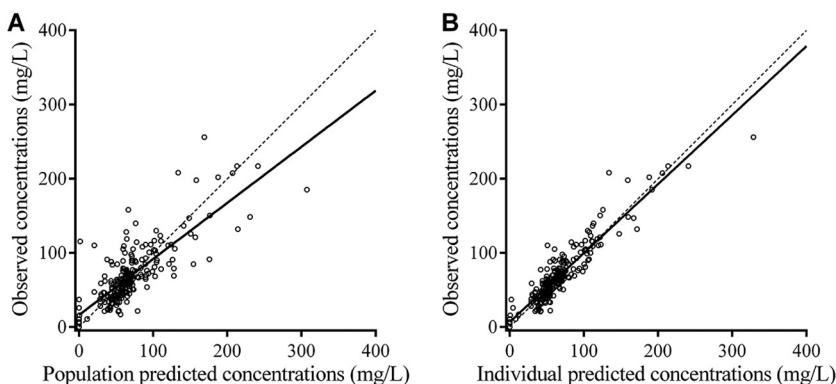


FIG 1 Observed versus population predicted cefazolin concentrations (A) and individual predicted cefazolin concentrations (B). The dashed lines represent identity. The full line is the linear regression line ($R^2 = 0.64$ for panel A and $R^2 = 0.86$ for panel B).

For the external data set, observed versus predicted concentration plots proved to be adequate (Fig. S3). Bias and imprecision were 0.280 and 1.07, respectively, for population predictions and 0.046 and 0.32, respectively, for individual predictions.

PTA and dosing nomogram. The dosing nomogram for cefazolin is presented in Fig. 3 and includes equations to directly calculate the daily dose required to achieve the targeted concentration with a PTA of 90%, given the patient’s aGFR. For example, for a cefazolin concentration target of 40 mg/liter and an aGFR at 30, 60, 90, and 120 ml/min, the daily dose needed to achieve a 100% $fT_{>4 \times MIC}$ ratio with a 90% success rate is 2.6, 4.3, 6.1, and 8.0 g/day, respectively.

DISCUSSION

The objective of this work was to use a population pharmacokinetic analysis in a population of patients with bacteremia and/or infective endocarditis to provide a dosing nomogram for cefazolin adaptation, considering renal function. Patient characteristics were heterogeneous, with a broad range of daily doses being administered (500 mg/day to 12,000 mg/day), considering *a priori* and *a posteriori* dose adaptation.

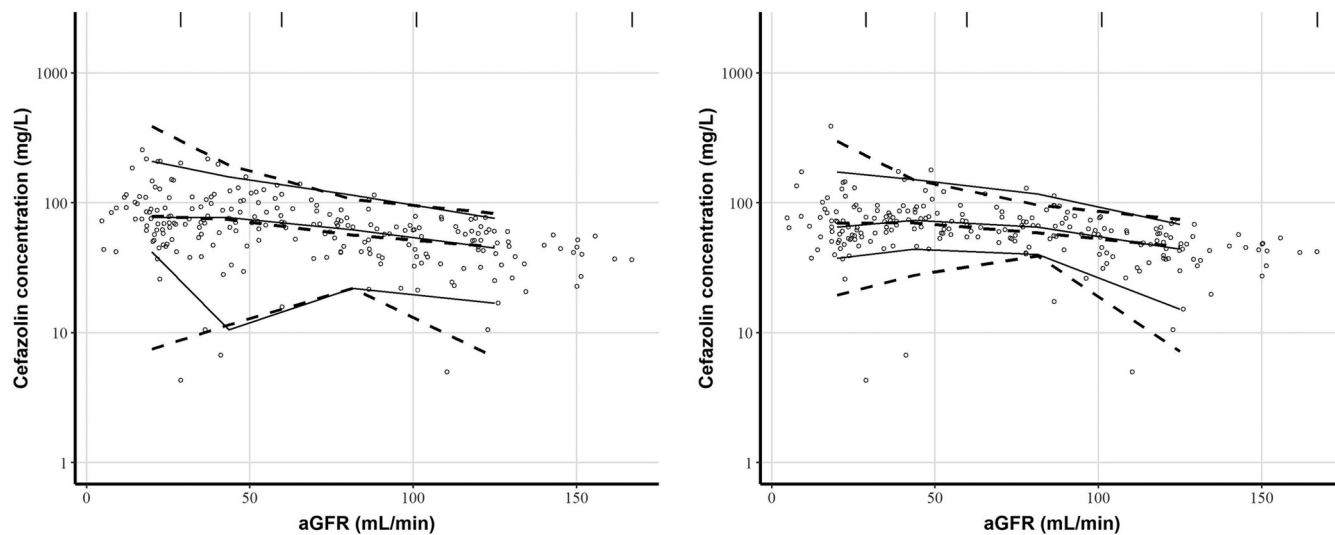


FIG 2 Visual predictive checks (left) and prediction-corrected visual predictive checks (right) of cefazolin concentrations against absolute values of the glomerular filtration rate (aGFR). Open circles are observed cefazolin concentrations. Solid lines represent the 5th, 50th, and 95th percentiles for observed concentrations. Dashed lines represent the 5th, 50th, and 95th percentiles for simulated concentrations. The vertical lines at the top of the plots are bin separators.

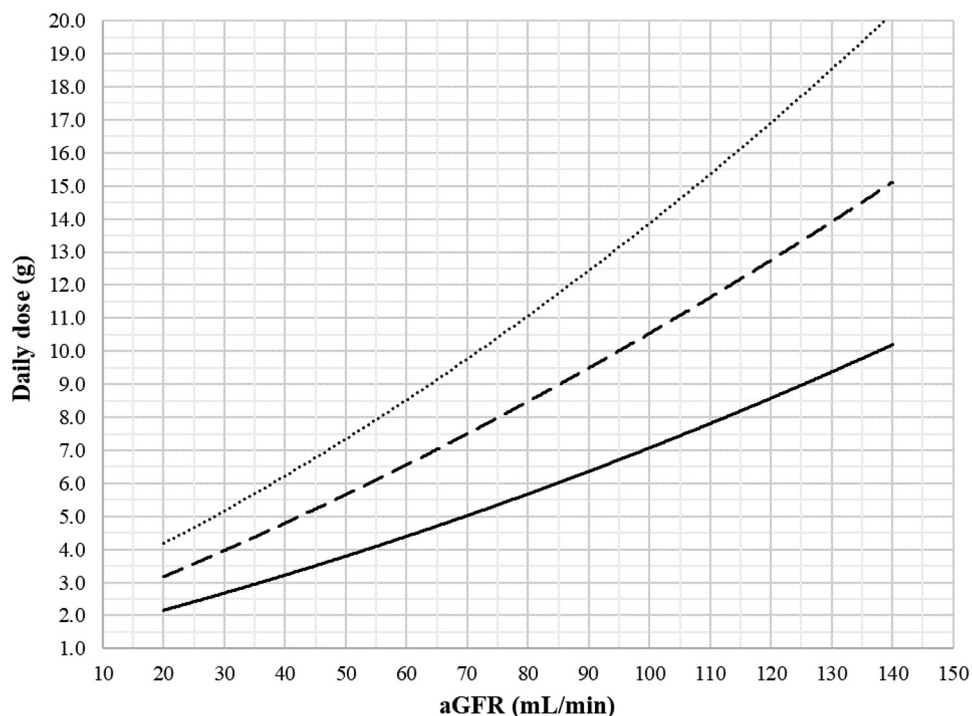


FIG 3 Nomogram of the daily dose of continuous-infusion cefazolin to be administered after a loading dose to attain steady-state plasma concentration targets of 40 mg/liter (full line), 60 mg/liter (dashed line), and 80 mg/liter (dotted line) in 90% of the studied population, accounting for renal function estimated by the CKD-EPI formula and expressed as an absolute value (aGFR). Equations were defined as $y = 0.0001x^2 + 0.448x + 1.2112$ for the 40-mg/liter target, $y = 0.0002x^2 + 0.0699x + 1.705$ for the 60-mg/liter target, and $y = 0.0003x^2 + 0.0837x + 2.3808$ for the 80-mg/liter target, with x being the aGFR and y being the cefazolin daily dose.

In previous works, cefazolin pharmacokinetics were simulated with models with two or more compartments and with cefazolin administration as an intravenous bolus (11–14). In our study, the one-compartment model was selected because of the continuous-infusion administration, which allowed cefazolin to reach steady state and thus achieve equilibrium between the central and peripheral compartments (15).

Similar to previous works, renal function estimation was found to have a strong impact on cefazolin pharmacokinetics (11–13). The Chronic Kidney Disease Epidemiology Collaboration (CKD-EPI) formula was used as the estimator of the glomerular filtration rate (GFR) because it is more accurate overall (16–18). However, the GFR estimated by the CKD-EPI formula is indexed by body surface area (BSA). While this normalization is useful for allowing comparisons between populations, it can be misleading at the individual level for patients with a BSA outside the normal range, where larger differences between the indexed value and the absolute value can be observed (19). The National Kidney Disease Education Program recommends the calculation of aGFR for drug dosing considerations (<https://www.niddk.nih.gov/health-information/professionals/clinical-tools-patient-education-outreach/ckd-drug-dosing-providers>). In this work, the patients had BSAs ranging from 1.36 to 2.56 m². Therefore, the use of aGFR instead of eGFR allowed for a better estimation of the renal elimination of cefazolin. This was confirmed by the pharmacokinetic modeling, where aGFR proved to be a better covariate than eGFR for the elimination rate constant. Considering these results, patients with impaired renal function should be treated carefully, given that delayed cefazolin clearance can lead to higher plasma concentrations and therefore increases in the risk of neurological toxicity (20). On the other hand, a high GFR can accelerate cefazolin elimination and lead to treatment failure. Therefore, the initial dosage should be adapted accordingly (21). It is important to keep in mind that aGFR is an estimator of renal function in the context of drug clearance and does not reflect either chronic or acute kidney injury.

Several studies have found a relationship between total body weight and the volume of the central compartment (11, 13, 22). In this work, we did not find such an association. In morbidly obese patients, the volume of the central compartment ranges from 7.06 liters to 13.0 liters, whereas in studies including patients with lower weights, values from 4.04 liters to 8.94 liters have been reported (11–13, 22, 23). Our estimate (3.19 liters) is close to the latter values.

Several limitations are present in this work. First, the data were gathered retrospectively from routine clinical practice and, thus, were more susceptible to imprecision. Furthermore, no data on clinical success or failure or on the MICs for the targeted bacteria were collected. Second, cefazolin free fractions were not measured. An 80% protein-bound fraction was used, based on the literature, but data suggest that the binding of cefazolin to proteins is saturable, with a higher proportion of the free fraction being detected when the total cefazolin concentration increases (24). Moreover, it remains to be determined whether the serum albumin concentration has an influence on the cefazolin free fraction. For patients with severe hypoproteinemia, the applicability of the model developed in this work remains to be determined, and thus, caution is advised when treating these patients. In addition, no gold standard measurement of renal function was performed in this study, and renal function assessment relied on estimators. Finally, a prospective evaluation of the nomogram should also be performed to assess its efficacy.

The aGFR parameter is important to consider when initiating cefazolin treatment. However, determining the optimal dose can be difficult. Dosing nomograms are simple tools that can provide the clinician a quick answer to this question of the optimal dose. Several nomograms have been established for multiple antibiotics, like vancomycin or gentamicin, but to our knowledge, there are no existing nomograms for cefazolin or for other β -lactam antibiotics (with the exception of meropenem) (25–28).

When we compared cefazolin dosing recommendations with the present nomogram, multiple observations could be made: for a 6,000-mg/day dose, PTA will be less than 90% for the 40-mg/liter target when a patient's aGFR is greater than 89 ml/min. Conversely, for patients with an aGFR of less than 38 ml/min, the probability that the concentration will be at least 80 mg/liter (associated with a higher risk of toxicity) is greater than 90%. In the same manner, the application of the French guidelines (80 to 100 mg/kg/day) to the dosing nomogram highlights the risk of underdosing for a patient weighing 73 kg (the median for the population studied) when aGFR is greater than 109 ml/min and the risk of toxicity when aGFR is less than 37 ml/min.

Since simulations for the conception of the nomogram were performed at steady state, the influence of giving a loading dose of cefazolin prior to the start of the continuous infusion was not assessed. However, given the short half-life of cefazolin (about 2 h) (29), steady state should be attained within 12 h after the start of the infusion, whether or not a loading dose is administered, allowing for therapeutic drug monitoring (TDM) early after the start of treatment.

Lastly, the nomogram should be used only with patients whose characteristics fall into those for the population with which the model was developed. In particular, patients with an aGFR of <20 ml/min or >140 ml/min or an extreme body weight (body mass index [BMI], <15 kg/m² or >35 kg/m²) should be managed with caution.

Conclusions. This nomogram can be a useful tool for physicians to assist with the individualization of the initial prescription of cefazolin in patients with infective endocarditis or bacteremia, with the systematic calculation of aGFR being a requirement. After treatment initiation, TDM should be used to adapt the dose regimen for each patient regardless of renal function.

MATERIALS AND METHODS

Patient population and data collection. Cefazolin concentration data were collected retrospectively from January 2013 to September 2018 from adult patients hospitalized in the Nantes University Hospital and treated with cefazolin, administered by continuous infusion, for bacteremia or infective endocarditis, followed by therapeutic drug monitoring (TDM). Patients who received any type of dialysis during treatment were excluded.

Data were split into two data sets: one that was used for model development and that included data for richly sampled patients and one that was used for external model validation and that was mostly composed of data from patients with few samples.

For each concentration data point, the dosage, duration of treatment, age, height, weight, and serum creatinine concentration were collected. When available, data on loading doses were also gathered. Multiple parameters were calculated: body mass index (BMI), body surface area (BSA) according to the Du Bois formula (30), lean body weight (LBW) according to the Devine formula (31), ideal weight (IWR) according to the Robinson formula (32), estimated glomerular filtration rate indexed by BSA (eGFR) according to the CKD-EPI formula (16), and the absolute value of the glomerular filtration rate (aGFR), calculated from the patient's eGFR and BSA.

To compare the population characteristics of the two data sets, Fisher's exact test and the Mann-Whitney-Wilcoxon test were performed using GraphPad Prism (version 6.01) software for Windows (GraphPad Software, La Jolla, CA, USA). The significance level was set to 0.05.

The study design was approved by the local human research and ethics committee of Nantes, France, on 23 April 2018 and was in accordance with French legislation (CNIL MR003).

Cefazolin quantitation. Total cefazolin plasma concentrations were determined by a validated high-performance liquid chromatography (HPLC) coupled with UV spectrometry (HPLC-UV) assay. Blood samples were collected in EDTA tubes and centrifuged ($1,500 \times g$ for 10 min at 4°C) upon reception at the laboratory. Plasma was retrieved and mixed with 1 ml of acetonitrile for protein precipitation. The mixture was then centrifuged ($1,800 \times g$ for 5 min at 4°C), and 1.6 ml of the supernatant layer was mixed with 8 ml of dichloromethane for extraction. The tubes were shaken horizontally for 10 min and centrifuged ($1,800 \times g$ for 5 min at 4°C). Fifty microliters of the upper aqueous layer was injected into the HPLC system (Agilent 1200 series; Agilent, Palo Alto, CA). The separation was performed on a Symmetry C_{18} 5- μm -particle-size column (250 by 4.6 mm [inner diameter]; Waters, Milford, MA). The UV absorbance peak for cefazolin was detected at 265 nm.

The lower limit of quantitation (LLOQ) of the method was 3 mg/liter. Accuracy was satisfactory, with intraday and interday coefficients of variation being less than 15% (20% for the LLOQ). Imprecision was also less than 15% (20% for the LLOQ).

Population pharmacokinetics analysis. (i) Structural model. The first data set was used to establish the structural model. Population pharmacokinetic modeling was performed using the non-parametric adaptive grid (NPAG) algorithm with the Pmetrics package for R (version 1.5.1) (33, 34).

One-compartment and two-compartment (central and peripheral) structural models with or without nonrenal elimination were initially tested without covariates to determine the best-fitting structural model and to estimate the parameters. Structural model selection was performed by evaluating the goodness of fit based on the Akaike information criterion (AIC), which is an estimate of the likelihood that the model is penalized by the number of parameters in the model. A lower value of the AIC indicates a better-fitting model. The models were also assessed by using population bias (the mean weighted error of predictions minus observations) and imprecision (the bias-adjusted mean weighted squared error of predictions minus observations) calculations and by using diagnostic plots: observed concentrations versus population and individually predicted concentrations and weighted residual versus time or individual predictions.

Additive and multiplicative error models were tested, where observations were weighted by $(\text{SD}^2 + \lambda^2)^{0.5}$ and $\text{SD} \times \gamma$, respectively, where λ and γ represent process noise, such as sampling time uncertainty and model misspecification. SD was the standard deviation of each observation, modeled by a polynomial equation: $C_0 + C_1 \times [\text{obs}] + C_2 \times [\text{obs}]^2 + C_3 \times [\text{obs}]^3$, where [obs] is the observed concentration.

The relationship between the model parameters and the different covariates (age, height, weight, serum creatinine, BMI, BSA, LBW, IWR, eGFR, aGFR) was then evaluated using stepwise linear regression and visual assessment of plots of the model parameters against covariates. The influence of body size-related covariates (height, weight, BMI, BSA, LBW, IWR) on compartmental volumes was tested, and the influence of renal function-related covariates (serum creatinine, eGFR, aGFR) on elimination parameters was tested on elimination parameters. The relation was evaluated by integrating the covariates in the model using either a linear [$P = P_1 + P_2 \times (\text{COV}/\text{COV}_{\text{median}})$], exponential [$P = P_1 \times e^{(P_2 \times \text{COV})/\text{COV}_{\text{median}}}$], power [$P = P_1 \times (\text{COV}/\text{COV}_{\text{median}})^{P_2}$], or allometric [$P = P_1 \times (\text{COV}/\text{COV}_{\text{median}})^{0.75}$] relationship for the influence of weight on distribution volumes, where P , P_1 , and P_2 are parameters; COV is the covariate value; and $\text{COV}_{\text{median}}$ is the covariate median in the data set. Covariates which improved population bias (mean weighted error of predictions minus observations) and imprecision (bias-adjusted mean weighted squared error of predictions minus observations) were integrated in the final model.

Parameter ranges were initially set wide and then narrowed when a candidate model was fit to increase the density of support points in the pertinent range.

The process was iterated until no further improvement to the model was observed.

(ii) Model validation. Visual predictive checks (VPC) and prediction-corrected visual predictive checks (pcVPC) were performed using Monte Carlo simulations ($n = 100$) from each patient in the first data set. Medians and 5th and 95th percentiles for observed and simulated concentrations were then compared visually. Plotting was done using the vpc package for R.

A zero-cycle run with the NPAG algorithm was used on the second data set with the tested model and prior support points from the first data set, and population bias and imprecision for this second population were retrieved and compared to those for the first population.

(iii) Probability of target attainment and dosing nomogram. Based on the parameters of the structural model, Monte Carlo simulations ($n = 1,000$) were generated from the patient profiles with various aGFR reflective of the population observed. For each of these profiles, exposure to cefazolin was

assessed for doses ranging from 500 mg/day to 50,000 mg/day, administered as a continuous infusion with a loading dose.

Targeted plasma concentrations for total cefazolin were defined as 40 mg/liter, 60 mg/liter, and 80 mg/liter. For the 2-mg/liter EUCAST epidemiological cutoff MIC for *S. aureus* (<https://mic.eucast.org/Eucast2/SearchController/search.jsp?action=performSearch&BeginIndex=0&Micdif=mic&NumberIndex=50&Antib=237&Specium=-1>), the most commonly isolated bacterium in our population, according to the 100% $f_{T > 4 \times \text{MIC}}$ ratio for efficacy (9) and the assumption that the free fraction is 20% of the total concentration (23, 35), the targeted total concentration should be at least 40 mg/liter at steady state. The 60-mg/liter target accounts for other *Staphylococcus* species for which no breakpoints have been defined but for which higher MICs can be encountered. The 80-mg/liter target was defined as an upper limit beyond which the toxicity risk can largely be increased and corresponds to a free drug concentration 8 times higher than the MIC, where the efficacy of β -lactams does not seem to be improved but neurotoxicity risk is increased (9, 36, 37).

To conceive the dosing nomogram, the lowest dose required to achieve a probability of target attainment (PTA) of 90% at steady state after a loading dose for each of the simulated patient profiles was reported against aGFR on a graph in Microsoft Excel software (Microsoft Corporation, Redmond WA, USA) for the 40-mg/liter, 60-mg/liter, and 80-mg/liter thresholds.

SUPPLEMENTAL MATERIAL

Supplemental material for this article may be found at <https://doi.org/10.1128/AAC.00806-19>.

SUPPLEMENTAL FILE 1, PDF file, 0.5 MB.

ACKNOWLEDGMENTS

This research received no specific grant from any funding agency in the public, commercial, or not-for-profit sectors.

We gratefully acknowledge Thierry Bompil for his advice.

REFERENCES

1. Selton-Suty C, Célard M, Le Moing V, Doco-Lecompte T, Chirouze C, lung B, Strady C, Revest M, Vandenesch F, Bouvet A, Delahaye F, Alla F, Duval X, Hoen B, APEPI Study Group. 2012. Preeminence of *Staphylococcus aureus* in infective endocarditis: a 1-year population-based survey. *Clin Infect Dis* 54:1230–1239. <https://doi.org/10.1093/cid/cis199>.
2. Asgeirsson H, Thalme A, Weiland O. 2018. *Staphylococcus aureus* bacteraemia and endocarditis—epidemiology and outcome: a review. *Infect Dis (Lond)* 50:175–192. <https://doi.org/10.1080/23744235.2017.1392039>.
3. Habib G, Lancellotti P, Antunes MJ, Bongiorni MG, Casalta J-P, Del Zotti F, Dulgheru R, El Khoury G, Erba PA, lung B, Miro JM, Mulder BJ, Plonska-Gosciniak E, Price S, Roos-Hesselinck J, Snygg-Martin U, Thuny F, Tornos Mas P, Vilacosta I, Zamorano JL. 2015. 2015 ESC guidelines for the management of infective endocarditis: The Task Force for the Management of Infective Endocarditis of the European Society of Cardiology (ESC) Endorsed by: European Association for Cardio-Thoracic Surgery (EACTS), the European Association of Nuclear Medicine (EANM). *Eur Heart J* 36:3075–3128. <https://doi.org/10.1093/eurheartj/ehv319>.
4. Baddour LM, Wilson WR, Bayer AS, Fowler VG, Tleyjeh IM, Rybak MJ, Barsic B, Lockhart PB, Gewitz MH, Levison ME, Bolger AF, Steckelberg JM, Baltimore RS, Fink AM, O'Gara P, Taubert KA, American Heart Association Committee on Rheumatic Fever, Endocarditis, and Kawasaki Disease of the Council on Cardiovascular Disease in the Young, Council on Clinical Cardiology, Council on Cardiovascular Surgery and Anesthesia, and Stroke Council. 2015. Infective endocarditis in adults: diagnosis, antimicrobial therapy, and management of complications: a scientific statement for healthcare professionals from the American Heart Association. *Circulation* 132: 1435–1486. <https://doi.org/10.1161/CIR.0000000000000296>.
5. McDanel JS, Roghmann M-C, Perencevich EN, Ohi ME, Goto M, Livorsi DJ, Jones M, Albertson JP, Nair R, O'Shea AMJ, Schweizer ML. 2017. Comparative effectiveness of cefazolin versus nafcillin or oxacillin for treatment of methicillin-susceptible *Staphylococcus aureus* infections complicated by bacteremia: a nationwide cohort study. *Clin Infect Dis* 65: 100–106. <https://doi.org/10.1093/cid/cix287>.
6. Bidell MR, Patel N, O'Donnell JN. 2018. Optimal treatment of MSSA bacteraemias: a meta-analysis of cefazolin versus antistaphylococcal penicillins. *J Antimicrob Chemother* 73:2643–2651. <https://doi.org/10.1093/jac/dky259>.
7. Roberts JA, Paul SK, Akova M, Bassetti M, De Waele JJ, Dimopoulos G, Kaukonen K-M, Koulenti D, Martin C, Montravers P, Rello J, Rhodes A, Starr T, Wallis SC, Lipman J, Roberts JA, Lipman J, Starr T, Wallis SC, Paul SK, Margarit Ribas A, De Waele JJ, De Crop L, Spapen H, Wauters J, Dugernier T, Jorens P, Dapper I, De Backer D, Taccone FS, Rello J, Ruano L, Afonso E, Alvarez-Lerma F, Gracia-Arnillas MP, Fernandez F, Feijoo N, Bardolet N, Rovira A, Garro P, Colon D, Castillo C, Fernando J, Lopez MJ, Fernandez JL, Arribas AM, Teja JL, Ots E, Carlos Montejo J, Catalan M, et al. 2014. DALI: defining antibiotic levels in intensive care unit patients: are current β -lactam antibiotic doses sufficient for critically ill patients? *Clin Infect Dis* 58:1072–1083. <https://doi.org/10.1093/cid/ciu027>.
8. Tam VH, McKinnon PS, Akins RL, Rybak MJ, Drusano GL. 2002. Pharmacodynamics of cefepime in patients with Gram-negative infections. *J Antimicrob Chemother* 50:425–428. <https://doi.org/10.1093/jac/dkf130>.
9. Guilhaumou R, Benaboud S, Bennis Y, Dahyot-Fizelier C, Dailly E, Gandia P, Goutelle S, Lefeuvre S, Mongardon N, Roger C, Scala-Bertola J, Lemaitre F, Garnier M. 2019. Optimization of the treatment with beta-lactam antibiotics in critically ill patients—guidelines from the French Society of Pharmacology and Therapeutics (Société Française de Pharmacologie et Thérapeutique—SFPT) and the French Society of Anaesthesia and Intensive Care Medicine (Société Française d'Anesthésie et Réanimation—SFAR). *Crit Care* 23:104. <https://doi.org/10.1186/s13054-019-2378-9>.
10. Jacobs A, Taccone FS, Roberts JA, Jacobs F, Cotton F, Wolff F, Creteur J, Vincent J-L, Hites M. 2018. β -Lactam dosage regimens in septic patients with augmented renal clearance. *Antimicrob Agents Chemother* 62: e02534-17. <https://doi.org/10.1128/AAC.02534-17>.
11. Naik BI, Roger C, Ikeda K, Todorovic MS, Wallis SC, Lipman J, Roberts JA. 2017. Comparative total and unbound pharmacokinetics of cefazolin administered by bolus versus continuous infusion in patients undergoing major surgery: a randomized controlled trial. *Br J Anaesth* 118: 876–882. <https://doi.org/10.1093/bja/aex026>.
12. Grégoire M, Dumont R, Ronchi L, Woillard J-B, Atthar V, Letessier E, Cinotti R, Roquilly A, Deslandes G, Jolliet P, Asehnoune K, Dailly E. 2018. Prophylactic cefazolin concentrations in morbidly obese patients undergoing sleeve gastrectomy: do we achieve targets? *Int J Antimicrob Agents* 52:28–34. <https://doi.org/10.1016/j.ijantimicag.2018.02.015>.
13. Roberts JA, Udy AA, Jarrett P, Wallis SC, Hope WW, Sharma R, Kirkpatrick CMJ, Kruger PS, Roberts MS, Lipman J. 2015. Plasma and target-site subcutaneous tissue population pharmacokinetics and dosing simula-

- tions of cefazolin in post-trauma critically ill patients. *J Antimicrob Chemother* 70:1495–1502. <https://doi.org/10.1093/jac/dku564>.
14. Dallmann A, Ince I, Solodenko J, Meyer M, Willmann S, Eissing T, Hempel G. 2017. Physiologically based pharmacokinetic modeling of renally cleared drugs in pregnant women. *Clin Pharmacokinet* 56:1525–1541. <https://doi.org/10.1007/s40262-017-0538-0>.
 15. Zheng H. 2015. Intravenous infusion, p. 150–167. In Shargel L, Yu ABC (ed), *Applied biopharmaceutics & pharmacokinetics*, 7th ed. McGraw-Hill Education, New York, NY.
 16. Levey AS, Stevens LA, Schmid CH, Zhang YL, Castro AF, Feldman HI, Kusek JW, Eggers P, Van Lente F, Greene T, Coresh J. 2009. A new equation to estimate glomerular filtration rate. *Ann Intern Med* 150:604–612. <https://doi.org/10.7326/0003-4819-150-9-200905050-00006>.
 17. White CA, Akbari A, Doucette S, Fergusson D, Knoll GA. 2010. Estimating glomerular filtration rate in kidney transplantation: is the new chronic kidney disease epidemiology collaboration equation any better? *Clin Chem* 56:474–477. <https://doi.org/10.1373/clinchem.2009.135111>.
 18. Michels WM, Grootendorst DC, Verduijn M, Elliott EG, Dekker FW, Krediet RT. 2010. Performance of the Cockcroft-Gault, MDRD, and new CKD-EPI formulas in relation to GFR, age, and body size. *Clin J Am Soc Nephrol* 5:1003–1009. <https://doi.org/10.2215/CJN.06870909>.
 19. Redal-Baigorri B, Rasmussen K, Heaf JG. 2013. The use of absolute values improves performance of estimation formulae: a retrospective cross sectional study. *BMC Nephrol* 14:271. <https://doi.org/10.1186/1471-2369-14-271>.
 20. Chow KM, Hui AC, Szeto CC. 2005. Neurotoxicity induced by beta-lactam antibiotics: from bench to bedside. *Eur J Clin Microbiol Infect Dis* 24:649–653. <https://doi.org/10.1007/s10096-005-0021-y>.
 21. Carrié C, Petit L, d'Houdain N, Sauvage N, Cottenceau V, Lafitte M, Founteize C, Hisz Q, Menu D, Legeron R, Breilh D, Sztark F. 2018. Association between augmented renal clearance, antibiotic exposure and clinical outcome in critically ill septic patients receiving high doses of β -lactams administered by continuous infusion: a prospective observational study. *Int J Antimicrob Agents* 51:443–449. <https://doi.org/10.1016/j.ijantimicag.2017.11.013>.
 22. Brill MJE, Houwink API, Schmidt S, Van Dongen EPA, Hazebroek EJ, van Ramshorst B, Deneer VH, Mouton JW, Knibbe C. 2014. Reduced subcutaneous tissue distribution of cefazolin in morbidly obese versus non-obese patients determined using clinical microdialysis. *J Antimicrob Chemother* 69:715–723. <https://doi.org/10.1093/jac/dkt444>.
 23. van Kralingen S, Taks M, Diepstraten J, van de Garde EM, van Dongen EP, Wiezer MJ, van Ramshorst B, Vlamincx B, Deneer VH, Knibbe CA. 2011. Pharmacokinetics and protein binding of cefazolin in morbidly obese patients. *Eur J Clin Pharmacol* 67:985–992. <https://doi.org/10.1007/s00228-011-1048-x>.
 24. Vella-Brincat JWA, Begg EJ, Kirkpatrick CMJ, Zhang M, Chambers ST, Gallagher K. 2007. Protein binding of cefazolin is saturable in vivo both between and within patients. *Br J Clin Pharmacol* 63:753–757. <https://doi.org/10.1111/j.1365-2125.2006.02827.x>.
 25. Minichmayr IK, Roberts JA, Frey OR, Roehr AC, Kloft C, Brinkmann A. 2018. Development of a dosing nomogram for continuous-infusion meropenem in critically ill patients based on a validated population pharmacokinetic model. *J Antimicrob Chemother* 73:1330–1339. <https://doi.org/10.1093/jac/dkx526>.
 26. Pea F, Viale P, Cojutti P, Furlanut M. 2012. Dosing nomograms for attaining optimum concentrations of meropenem by continuous infusion in critically ill patients with severe gram-negative infections: a pharmacokinetics/pharmacodynamics-based approach. *Antimicrob Agents Chemother* 56:6343–6348. <https://doi.org/10.1128/AAC.01291-12>.
 27. Shino N, Uchida T, Yoshida M, Nomura Y. 2015. Development and assessment of a nomogram to propose the initial dosage regimen of a meropenem infusion based on serum creatinine and age using a Monte Carlo simulation. *Chem Pharm Bull (Tokyo)* 63:986–991. <https://doi.org/10.1248/cpb.c15-00494>.
 28. Roberts JA, Kumar A, Lipman J. 2017. Right dose, right now: customized drug dosing in the critically ill. *Crit Care Med* 45:331–336. <https://doi.org/10.1097/CCM.0000000000002210>.
 29. Bergan T, Brodwall EK, Ørjavik O. 1977. Pharmacokinetics of cefazolin in patients with normal and impaired renal function. *J Antimicrob Chemother* 3:435–443. <https://doi.org/10.1093/jac/3.5.435>.
 30. Du Bois D, Du Bois EF. 1916. A formula to estimate the approximate surface area if height and weight be known. *Arch Intern Med (Chic)* XVII:863–871. <https://doi.org/10.1001/archinte.1916.00080130010002>.
 31. Devine BJ. 1974. Gentamicin therapy. *Ann Pharmacother* 8:650–655.
 32. Robinson JD, Lupkiewicz SM, Palenik L, Lopez LM, Ariet M. 1983. Determination of ideal body weight for drug dosage calculations. *Am J Hosp Pharm* 40:1016–1019.
 33. Neely MN, van Guilder MG, Yamada WM, Schumitzky A, Jelliffe RW. 2012. Accurate detection of outliers and subpopulations with Pmetrics, a nonparametric and parametric pharmacometric modeling and simulation package for R. *Ther Drug Monit* 34:467–476. <https://doi.org/10.1097/FTD.0b013e31825c4ba6>.
 34. R Core Team. 2018. R: a language and environment for statistical computing. R Foundation for Statistical Computing, Vienna, Austria.
 35. Wong G, Briscoe S, Adnan S, McWhinney B, Ungerer J, Lipman J, Roberts JA. 2013. Protein binding of β -lactam antibiotics in critically ill patients: can we successfully predict unbound concentrations? *Antimicrob Agents Chemother* 57:6165–6170. <https://doi.org/10.1128/AAC.00951-13>.
 36. Manduru M, Mihm LB, White RL, Friedrich LV, Flume PA, Bosso JA. 1997. In vitro pharmacodynamics of ceftazidime against *Pseudomonas aeruginosa* isolates from cystic fibrosis patients. *Antimicrob Agents Chemother* 41:2053–2056. <https://doi.org/10.1128/AAC.41.9.2053>.
 37. Beumier M, Casu GS, Hites M, Wolff F, Cotton F, Vincent JL, Jacobs F, Taccone FS. 2015. Elevated β -lactam concentrations associated with neurological deterioration in ICU septic patients. *Minerva Anestesiol* 81:497–506.